Available online at www.sciencedirect.com
SCIENCE DIRECT®
ELSEVIER
International Journal of Solids and Structures 42 (2005) 6610–6627
INTERNATIONAL JOURNAL OF SOLIDS and STRUCTURES
www.elsevier.com/locate/ijsolstr

Wavelet packet based damage identification of beam structures

Jian-Gang Han [a], Wei-Xin Ren [a,b,*], Zeng-Shou Sun [a]

[a] *Department of Civil Engineering, Fuzhou University, Fuzhou, Fujian 350002, People's Republic of China*
[b] *Department of Civil Engineering, Central South University, Changsha, Hunan 410075, People's Republic of China*

Received 1 August 2004; received in revised form 6 April 2005
Available online 8 June 2005

Abstract

Most of vibration-based damage detection methods require the modal properties that are obtained from measured signals through the system identification techniques. However, the modal properties such as natural frequencies and mode shapes are not such a good sensitive indication of structural damage. The wavelet packet transform (WPT) is a mathematical tool that has a special advantage over the traditional Fourier transform in analyzing non-stationary signals. It adopts redundant basis functions and hence can provide an arbitrary time-frequency resolution. In this study, a damage detection index called wavelet packet energy rate index (WPERI), is proposed for the damage detection of beam structures. The measured dynamic signals are decomposed into the wavelet packet components and the wavelet energy rate index is computed to indicate the structural damage. The proposed damage identification method is firstly illustrated with a simulated simply supported beam and the identified damage is satisfactory with assumed damage. Afterward, the method is applied to the tested steel beams with three damage scenarios in the laboratory. Despite the noise is present for real measurement data, the identified damage pattern is comparable with the tests. Both simulated and experimental studies demonstrated that the WPT-based energy rate index is a good candidate index that is sensitive to structural local damage.
© 2005 Elsevier Ltd. All rights reserved.

Keywords: Damage detection; Wavelet packet transform; Energy rate index; Beam; Dynamic measurement; Signal process

1. Introduction

During the service of beam structures such as large-scale frames, long-span bridges and high-rise buildings, local damage of their key positions may continually accumulate, and finally results in sudden failure of

* Corresponding author. Address: Department of Civil Engineering, Fuzhou University, 523 Gongye Road, Fujian Province, Fuzhou 350002, China. Tel.: +86 591 8789 2454; fax: +86 591 8373 7442.
E-mail address: ren@fzu.edu.cn (W.-X. Ren).
URL: http://bridge.fzu.edu.cn (W.-X. Ren).

0020-7683/$ - see front matter © 2005 Elsevier Ltd. All rights reserved.
doi:10.1016/j.ijsolstr.2005.04.031

structures. One damage identification classification system commonly defines four levels of damage assessment (Doebling et al., 1998): (1) the presence of damage; (2) the location of the damage; (3) quantification of the severity of the damage; and (4) prediction of the remaining serviceability of the structure. Basically, damage identification techniques can be classified into either local or global methods. Most currently used techniques, such as visual, acoustic, magnetic field, eddy current, etc., are effective yet local in nature. They require that the vicinity of the damage is known a priori and the portion of the structure being inspected is readily assessable. The global damage identification methods, on the other hand, quantity the healthiness of a structure by examining changes in its global structural characteristics. It is believed that these two methods should be used in a complementary way to effectively and correctly assess the condition of the health of a complicated structure.

One core issue of the global vibration-based damage assessment methods is to seek some damage indices that are sensitive to structural damage (Ren and De Roeck, 2002a,b). The damage indices that have been demonstrated with various degrees of success include natural frequencies, mode shapes, mode shape curvatures, modal flexibility, modal strain energy, etc. Doebling et al. (1998) and Farrar et al. (1999) summarized the comprehensive historic development of damage assessment methodologies based on these indices as well as pointed out their applicability and limitations. Most of vibration-based damage assessment methods require the modal properties that are obtained from the measured signals through the system identification techniques such as the Fourier transform (FT). The structural damage is typically a local phenomenon, which tends to be captured by higher frequency signals. The Fourier analysis transforms the signal from a time-based or space-based domain to a frequency-based one. Unfortunately, the time or space information may be lost during performing such a transform and it is sometimes impossible to determine when or where a particular event took place. To correct this deficiency, the short-time Fourier transform (STFT) was proposed by Gabor (1946). This windowing technique analyzes only a small section of the signal at a time. The STFT maps a signal into a 2-D function of time or space and frequency. The transformation has the disadvantage that the information about time or space and frequency can be obtained with a limited precision that is determined by the size of the window. A higher resolution in time or space and frequency domain cannot be achieved simultaneously since once the window size is chosen, it is the same for all frequencies.

The wavelet transform (WT) is precisely a new way to analyze the signals, which overcomes the problems that other signal processing techniques exhibit. Wavelet functions are composed of a family of basis functions that are capable of describing a signal in a localized time (or space) and frequency (or scale) domain (Daubechies, 1992). The main advantage gained by using wavelets is the ability to perform local analysis of a signal, i.e., zooming on any interval of time or space. Wavelet analysis is thus capable of revealing some hidden aspects of the data that other signal analysis techniques fail to detect. This property is particularly important for damage detection applications. Many investigators (Wang and McFadden, 1996; Kitada, 1998; Gurley and Kareem, 1999; Wang and Deng, 1999; Hou et al., 2000; Ovanesova and Suarez, 2003) presented applications of wavelet transform to detect cracks in frame structures. One possible drawback of the WT is that the frequency resolution is quite poor in the higher frequency region. Hence, it still faces the difficulties when discriminating the signals containing close high frequency components.

The wavelet packet transform (WPT) is an extension of the WT, which provides a complete level-by-level decomposition of signal (Mallat, 1989). The wavelet packets are alternative bases formed by the linear combinations of the usual wavelet functions (Coifman and Wickerhauser, 1992). Therefore, the WPT enables the extraction of features from the signals that combine the stationary and non-stationary characteristics with an arbitrary time-frequency resolution. Sun and Chang (2002) developed a WPT-based component energy technique for analyzing structural damage. The component energies were firstly calculated and then they were used as inputs into the neural network (NN) models for damage assessment.

In this paper, a WPT-based method is proposed for the damage detection of beam structures. Dynamic signals measured from structures are first decomposed into the wavelet packet components. The wavelet energy rate index is proposed, which is then used to locate damage. Both simulated and tested beams with

different damage scenarios are used as the case studies to validate the applicability of proposed damage identification procedure. The results demonstrated that the WPT-based energy index is a good candidate index that is sensitive to structural local damage.

2. Theoretical background

Wavelet packets consist of a set of linearly combined usual wavelet functions. The wavelet packets inherit the properties such as orthonormality and time-frequency localization from their corresponding wavelet functions. A wavelet packet $\psi^i_{j,k}(t)$ is a function with three indices where integers i, j and k are the modulation, scale and translation parameters, respectively,

$$\psi^i_{j,k}(t) = 2^{j/2}\psi^j(2^j t - k), \quad i = 1, 2, 3, \ldots \tag{1}$$

The wavelet functions ψ^i can be obtained from the following recursive relationships:

$$\psi^{2j}(t) = \sqrt{2}\sum_{k=-\infty}^{\infty} h(k)\psi^i(2t-k), \tag{2}$$

$$\psi^{2j+1}(t) = \sqrt{2}\sum_{k=-\infty}^{\infty} g(k)\psi^i(2t-k). \tag{3}$$

The first wavelet is so-called a mother wavelet function as follows:

$$\psi^1(t) = \psi(t). \tag{4}$$

The discrete filters $h(k)$ and $g(k)$ are the quadrature mirror filters associated with the scaling function and the mother wavelet function. There are quite a few mother wavelets reported in the literature. Most of these mother wavelets are developed to satisfy some key properties such as the invertibility and orthogonality. Daubechies (1992) developed a family of mother wavelets based on the solution of a dilation equation. One of these wavelet functions, DB5, is adopted in this study.

The WT consists of one high frequency term from each level and one low-frequency residual from the last level of decomposition. The WPT, on the other hand, contains a complete decomposition at every level and hence can achieve a higher resolution in the high frequency region. The recursive relations between the jth and the $(j+1)$th level components are

$$f^i_j(t) = f^{2i-1}_{j+1}(t) + f^{2i}_{j+1}(t), \tag{5}$$

$$f^{2i-1}_{j+1}(t) = Hf^i_j(t), \tag{6}$$

$$f^{2i}_{j+1}(t) = Gf^i_j(t), \tag{7}$$

where H and G are the filtering-decimation operators related to the discrete filters $h(k)$ and $g(k)$ in such a way

$$H\{\cdot\} = \sum_{k=-\infty}^{\infty} h(k-2t), \tag{8}$$

$$G\{\cdot\} = \sum_{k=-\infty}^{\infty} g(k-2t). \tag{9}$$

After j level of decomposition, the original signal $f(t)$ can be expressed as

$$f(t) = \sum_{i=1}^{2^j} f^i_j(t). \tag{10}$$

The wavelet packet component signal $f_j^i(t)$ can be represented by a linear combination of wavelet packet functions $\psi_{j,k}^i(t)$ as follows:

$$f_j^i(t) = \sum_{k=-\infty}^{\infty} c_{j,k}^i(t)\psi_{j,k}^i(t), \tag{11}$$

where the wavelet packet coefficients $c_{j,k}^i(t)$ can be obtained from

$$c_{j,k}^i(t) = \int_{-\infty}^{\infty} f(t)\psi_{j,k}^i(t)\,\mathrm{d}t, \tag{12}$$

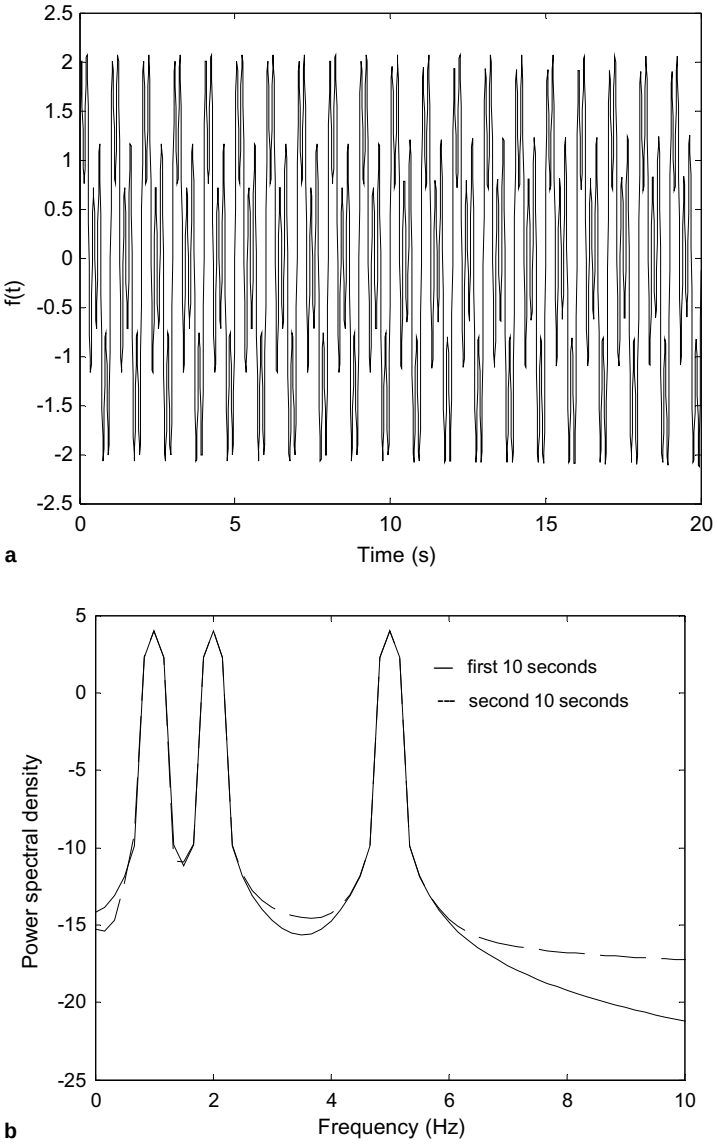

Fig. 1. Three-component harmonic function (a) and its power spectrum (b).

providing that the wavelet packet functions are orthogonal

$$\psi_{j,k}^{m}(t)\psi_{j,k}^{n}(t) = 0 \quad \text{if } m \neq n. \tag{13}$$

Each component in the WPT tree can be viewed as the output of a filter tuned to a particular basis function, thus the whole tree can be regarded as a filter bank. At the top of WPT tree (lower level), the WPT yields a good resolution in the time domain but a poor resolution in the frequency domain. At the bottom of WPT tree (higher level), the WPT results in a good resolution in the frequency domain yet a poor resolution in the time domain.

To illustrate the WPT, the following example is given:

$$f(t) = \begin{cases} \sin(2\pi t) + \sin(4\pi t) + \sin(10\pi t) & (0 \leqslant t \leqslant 10\ \text{s}), \\ \sin(1.998\pi t) + \sin(4\pi t) + \sin(10\pi t) & (10 < t \leqslant 20\ \text{s}). \end{cases} \tag{14}$$

This harmonic function as shown in Fig. 1(a) basically contains three frequencies: 1.0, 2.0, and 5.0 Hz up to 10 s. After 10 s, 1.0 Hz frequency is suddenly reduced to 0.999 Hz. Fig. 1(b) shows the FT results for the first 10 s and the last 10 s. As expected, the small perturbation of the 1.0 Hz frequency is not visible from the spectral density function by the FT. However, this small change in frequency can be detected by the WPT. Fig. 2 shows the eight wavelet packet component signals after three levels of wavelet packet decomposition. It can be seen that the suddenly shift at 10 s is quit visible in most of the wavelet component signals.

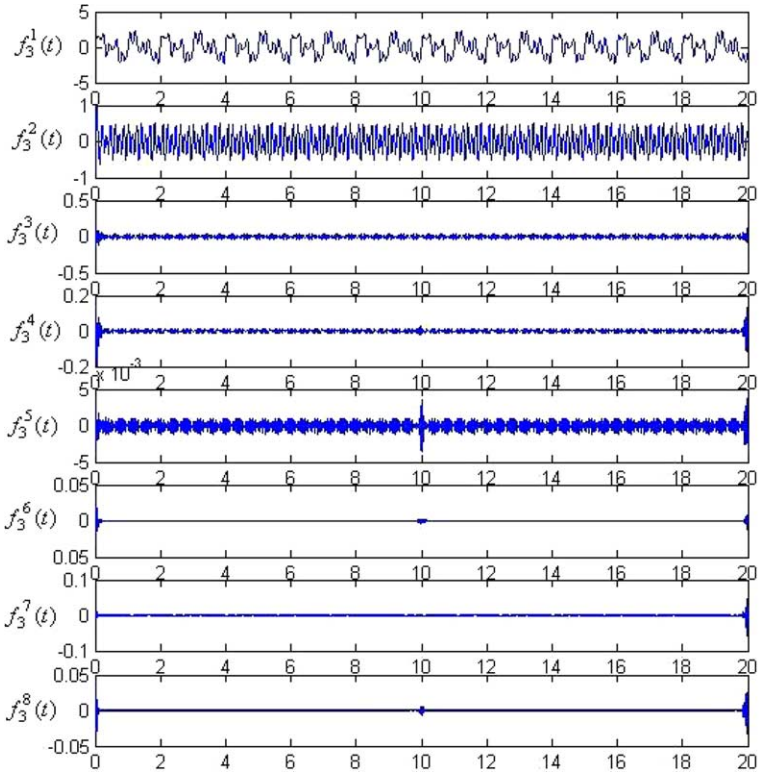

Fig. 2. Signal components of third level wavelet packet transform (WPT).

3. Wavelet packet energy rate index

Yen and Lin (2000) investigated the feasibility of applying the WPT to the vibration signals. They defined a wavelet packet node energy index and concluded that the node energy representation could provide a more robust signal feature for classification than using the wavelet packet coefficients directly. Sun and Chang (2002) proposed a wavelet packet component energy index which was then used as inputs of neural network models for damage assessment. The numerical simulations were performed using a three-span continuous bridge under impact excitation. Various levels of damage assessment including the occurrence, location, and severity of the damage were studied. In this study, the wavelet packet energy index is proposed to identify the locations and severity of damage. To do that, the signal energy E_f at j level is first defined as

$$E_{f_j} = \int_{-\infty}^{\infty} f^2(t)\,\mathrm{d}t = \sum_{m=1}^{2^j}\sum_{n=1}^{2^j}\int_{-\infty}^{\infty} f_j^m(t) f_j^n(t)\,\mathrm{d}t. \tag{15}$$

Substituting Eq. (11) into Eq. (15) and using the orthogonal condition Eq. (13) yields

$$E_{f_j} = \sum_{i=1}^{2^j} E_{f_j^i}, \tag{16}$$

where the wavelet packet component energy $E_{f_j^i}$ can be considered to be the energy stored in the component signal $f_j^i(t)$,

$$E_{f_j^i} = \int_{-\infty}^{\infty} f_j^i(t)^2\,\mathrm{d}t. \tag{17}$$

It can be seen that the component signal $f_j^i(t)$ is a superposition of wavelet functions $\psi_{j,k}^i(t)$ of the same scale as j but translated into the time domain ($-\infty < k < \infty$). This means that the component energy $E_{f_j^i}$ is the energy stored in a frequency band determined by the wavelet functions $\psi_{j,k}^i(t)$. Physically, Eq. (16) illustrates that the total signal energy can be decomposed into a summation of wavelet packet component energies that correspond to different frequency bands.

The component energies for the third level WPT before (denoted E_a) and after (denoted E_b) the frequency shift for the harmonic function Eq. (14) are listed in Table 1. Duration of 4 s is used for computing E_a within an interval of 2–6 s and E_b within a interval of 14–18 s, respectively. For comparison, the third level WT component energies and their changes are also calculated. It is demonstrated that both WT component energies and WPT component energies are not sensitive to the shift at this level of decomposition.

In fact, the signal energy is mainly contributed by the first (f_3^1) and the second (f_3^2) components. These two component energies are nearly close to the original signal energy. To further illustrate, the WT component energies and the first 20 WPT component energies of the fifth level decomposition are listed in Table 2. It can be observed that the component energies for the first two WT components are more sensitive to the original signal energy. The WPT component energies are even more sensitive than those of WT. Also it can be seen that those small-value component energies are more sensitive than the characteristics change, e.g., the energy change for f_5^4 and f_5^5 are 115.8% and 99.74%, respectively. Ideally, these sensitive component energies are good candidate indices that can reveal the signal characteristics. So the wavelet packet energy rate index (WPERI) is proposed to indicate the structural damage. The rate of signal wavelet packet energy $\Delta(E_{f_j})$ at j level is defined as

$$\Delta(E_{f_j}) = \sum_{i=1}^{2^j} \frac{\left|(E_{f_j^i})_b - (E_{f_j^i})_a\right|}{(E_{f_j^i})_a}, \tag{18}$$

Table 1
Component energies for the third level wavelet transform (WT) and wavelet packet transform (WPT) before (E_a) and after (E_b) shift in frequency of the harmonic function

		E_a (2–6 s)	E_b (14–18 s)	Change (%)
WT	$f(t)$	6.0	6.0087	0.15
	$f_3^a(t)$	5.6702	5.6790	0.16
	$f_3^d(t)$	0.3284	0.3284	0.00
	$f_2^d(t)$	0.0014	0.0014	0.00
	$f_1^d(t)$	2.0371e−6	2.0371e−6	0.00
WPT	$f(t)$	6.0	6.0087	0.15
	$f_3^1(t)$	5.6702	5.6790	0.16
	$f_3^2(t)$	0.3284	0.3284	0.00
	$f_3^3(t)$	0.0012	0.0012	0.00
	$f_3^4(t)$	0.0002	0.0002	0.00
	$f_3^5(t)$	1.7014e−6	1.7014e−6	0.00
	$f_3^6(t)$	3.3422e−7	3.3422e−7	0.00
	$f_3^7(t)$	1.224e−9	1.224e−9	0.00
	$f_3^8(t)$	2.4046e−10	2.4046e−10	0.00

Table 2
Component energies for the fifth level wavelet transform (WT) and wavelet packet transform (WPT) (first 20 terms) before (E_a) and after (E_b) shift in frequency of the harmonic function

		E_a (2–6 s)	E_b (14–18 s)	Change (%)
WT	$f(t)$	6.0	6.0087	0.15
	$f_5^a(t)$	2.0782	2.1887	5.3153
	$f_5^d(t)$	1.7523	1.8814	7.3677
	$f_4^d(t)$	1.7419	1.7419	0.00
	$f_3^d(t)$	0.32835	0.32835	0.00
	$f_2^d(t)$	0.0014382	0.0014382	0.00
	$f_1^d(t)$	2.0371e−006	2.0371e−006	0.00
WPT	$f(t)$	6.0	6.0087	0.15
	$f_5^1(t)$	2.0782	2.1887	5.3153
	$f_5^2(t)$	1.7523	1.8814	7.3677
	$f_5^3(t)$	1.5656	1.2371	−20.982
	$f_5^4(t)$	0.2157	0.46548	115.8
	$f_5^5(t)$	0.00014172	0.00028307	99.737
	$f_5^6(t)$	0.00028746	0.00011594	−59.668
	$f_5^7(t)$	0.28612	0.26205	−8.4136
	$f_5^8(t)$	0.051949	0.055757	7.3296
	$f_5^9(t)$	8.2926e−007	6.5244e−007	−21.322
	$f_5^{10}(t)$	2.4007e−007	4.4744e−007	86.377
	$f_5^{11}(t)$	0.001065	0.00094255	−11.494
	$f_5^{12}(t)$	0.00018429	0.00021012	14.012
	$f_5^{13}(t)$	1.4228e−007	1.4148e−007	−0.5645
	$f_5^{14}(t)$	2.8154e−008	2.7629e−008	−1.865
	$f_5^{15}(t)$	0.00021095	0.00018344	−13.042
	$f_5^{16}(t)$	3.6043e−005	4.1441e−005	14.977
	$f_5^{17}(t)$	1.1175e−009	9.657e−010	−13.587
	$f_5^{18}(t)$	1.7835e−010	6.4183e−010	259.87
	$f_5^{19}(t)$	1.4005e−006	1.4412e−006	2.9029
	$f_5^{20}(t)$	2.8151e−007	2.7678e−007	−1.6787

where $(E_{f_j^i})_a$ is the component signal energy $E_{f_j^i}$ at j level without damage, and $(E_{f_j^i})_b$ is the component signal energy $E_{f_j^i}$ with some damage. It is postulated that structural damage would affect the wavelet packet component energies and subsequently alter this damage indicator. It is desirable to select the WPERI that is sensitive to the changes in the signal characteristics.

4. Damage identification procedures

A damage identification procedure based on the proposed WPERI is described here. Two assumptions are adopted in this study: (1) the reliable undamaged and damaged structural models are available; (2) the structure is excited by the same impulse load and acts at the same location. Vibration signals measured from the structure by sensors are first processed using the WPT. The level of wavelet packet decomposition is determined through a trial and error sensitivity analysis using the undamaged and damaged structural models. Then the wavelet packet energy rates of signals are calculated.

It is proposed to establish threshold values for the damage indicators based on the statistical process control (SPC) method (Benffey, 1993; Montgomery, 1996). For structural health monitoring applications, Sohn et al. (2000) indicated that an X-bar control chart can provide a statistical framework for monitoring future measurements and for identifying abnormality in the new data. The core of the technique is in establishing the lower and upper control limits (LCL and UCL) that can enclose the variation of the extracted damage indicators due to measurement noise with a large probability. Hence, any damage indicator that falls outside of the enclosure signifies the change of the structural condition with high probability. Sun and Chang (2004) proposed two damage indicators for the purpose of structural health monitoring, which were then formulated to lump the discriminated information from the extracted wavelet packet signature. The thresholds for damage alarming were established using the statistical properties and the one-side confidence limit of the damage indicators from successive measurements.

If n stands for the total number of all sensors distributing in structure, a total of n WPERIs can be obtained after performing the wavelet packet decomposition. When the mean values and the standard deviations of these WPERIs are expressed as μ_{WPERI} and σ_{WPERI}, the one-side $(1-\alpha)$ upper confidence limit for the WPERI can be obtained from (Ang and Tang, 1975)

$$\mathrm{UL}^{\alpha}_{\mathrm{WPERI}} = \mu_{\mathrm{WPERI}} + Z_{\alpha}\left(\frac{\sigma_{\mathrm{WPERI}}}{\sqrt{n}}\right), \tag{19}$$

where Z_α is the value of a standard normal distribution with zero mean and unit variance such that the cumulative probability is $100(1-\alpha)\%$. This limit can be considered as a threshold value for alarming of possible abnormality in the damage indicator WPERI. One special advantage of this damage identification is that the setting of the threshold value is based on the statistical properties of the damage indicator measured with sensors. Any indicator that exceeds the threshold would cause damage alarming. So even when the multiple damage occurs, the proposed method can still work well. The location of sensors whose WPERI values exceed the threshold will indicate where possible damage occurs.

5. Simulated beams

To validate the applicability of the proposed wavelet packet based damage identification method, the simulated simply supported beams without damage and with several assumed damage elements are considered. The beam of 6 m length is discretized with 30 elements as shown in Fig. 3. The mass density and modulus of elasticity of material of beam are 2500 kg/m^3 and 3.2×10^4 MPa, respectively, while the area and

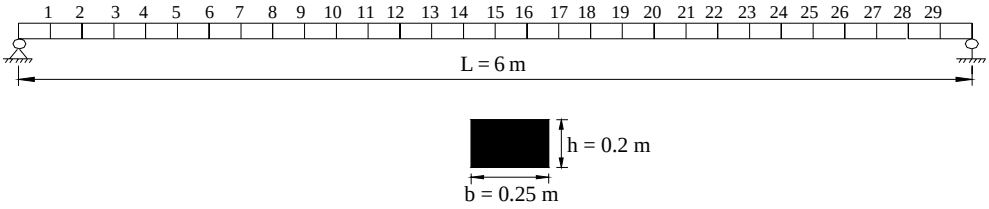

Fig. 3. A simulated simply supported beam.

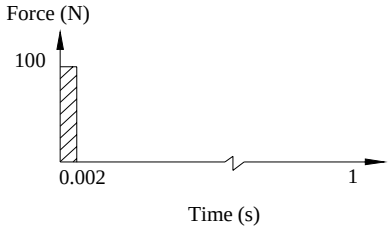

Fig. 4. Force–time history.

inertia moment of the cross section of simulated beam are 0.05 m^2 and 1.66×10^{-4} m^4, respectively. To emulate a practical impulse load, the force–time history as shown in Fig. 4 is applied at the distance 0.3 m from the left support of the beam. The node displacement responses of the beams under the impulse load are obtained by the finite element analysis package (ANSYS®, 1999) at a sampling frequency of 1000 Hz. Those displacement responses are regarded as the measured dynamic signals.

To simulate damage, four damage scenarios with different levels of severity and location are conceived. The damage severities are implemented by reducing the stiffness of specific elements. The reason to adopt this type of damage is that the damage could be easily emulated and quantified. The undamaged beam is denoted by D0 as a reference. The other four different damage scenarios, denoted as D1–D4, are described as follows: (1) D1: stiffness reduced 10% in the 15th and 16th elements; (2) D2: stiffness reduced 20% in the 15th and 16th elements; (3) D3: stiffness reduced 10% in the 8th, 9th, 15th and 16th elements; (4) D4: stiffness reduced 20% in the 8th, 9th, 15th and 16th elements.

A typical displacement response and its Fourier spectral density for the undamaged beam D0 are shown in Fig. 5, respectively. It can be shown that the node displacement responses generated by the impulse load are quite small. The first two natural frequencies below 200 Hz of the undamaged beam are found to be 35.989 and 143.18 Hz by the Fourier spectra. The first two natural frequencies for other four damage cases can also be found from their corresponding Fourier spectral density functions. These frequencies are list in Table 3. It is demonstrated that the damage results in the reduction of the beam natural frequencies. However, the changes of both frequencies for all damaged cases are less than 1.5% compared to those of undamaged case D0. Such a small change in natural frequencies indicates that the frequency index is not sensitive to the local structural damage.

The displacement responses of all damaged beams at the same node (node 10) are shown in Fig. 6. It can be observed that damage cannot been seen from the time history responses. As illustrated in the above example of the three-component harmonic function, a sufficiently high level of decomposition is required to obtain the sensitive component energies. For the simulated beams, the decomposition level is set to be 4 where a total of 16 component energies are generated. In order to study the effect of decomposition

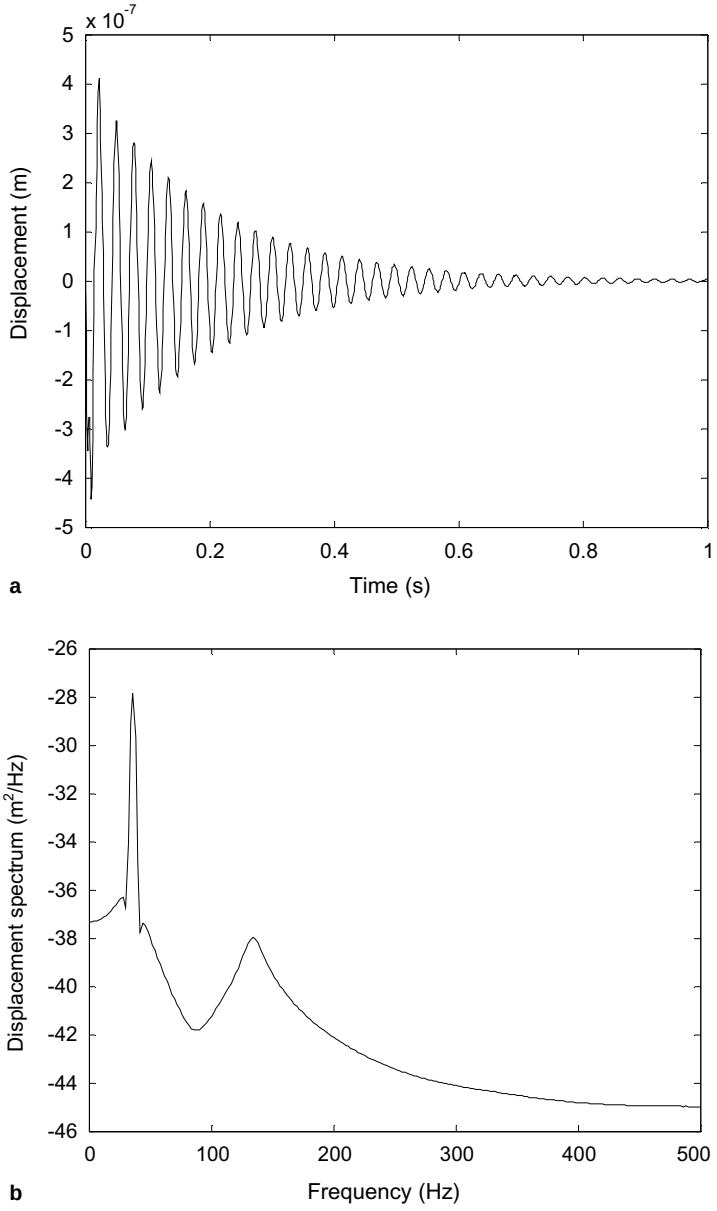

Fig. 5. Typical displacement response and its Fourier spectrum of undamaged beam.

Table 3
First two natural frequencies (Hz) for different damage scenarios

	D0	D1	D2	D3	D4
First mode	35.989	35.726	35.406	35.583	35.094
Second mode	143.18	143.16	143.14	142.15	140.90

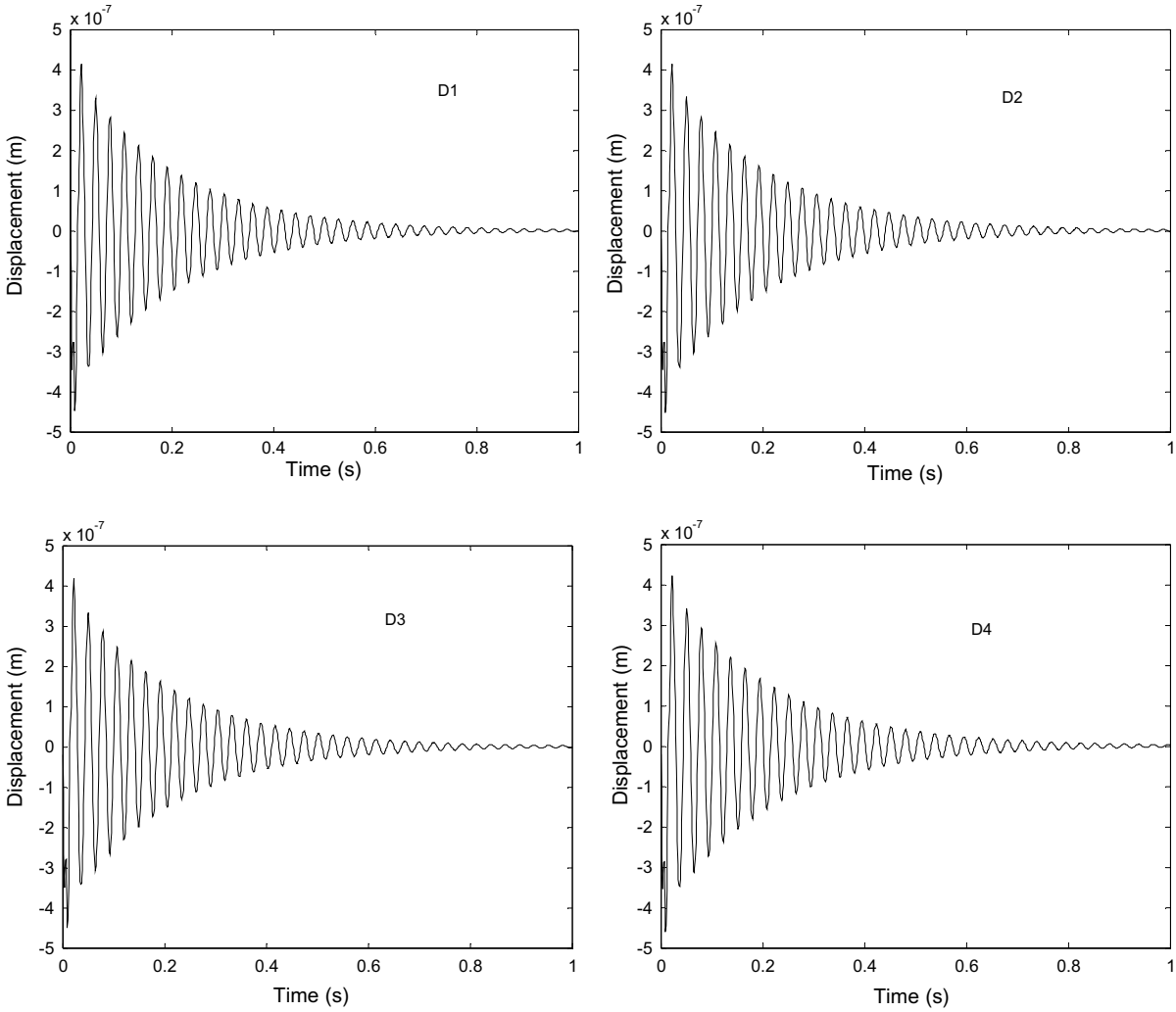

Fig. 6. Displacement responses at node 10 for different damaged beams.

level, the decomposition level is also set to be 5 where a total of 32 component energies are generated. It is found that both results seem very similar, which indicates that 4 decomposition level is enough. After decomposing the signals, the wavelet packet energy rate indices $\Delta(E_{fj})$ of each node are calculated using Eq. (18).

There are 29 WPERI $\Delta(E_{fj})$ values calculated for anyone damaged beam. The statistical analysis is then implemented within those 29 WPERI values. The mean value μ_{WPERI} and the standard deviation σ_{WPERI} can be calculated. Assuming that $\alpha = 0.02$, the one sided 98% confidence upper limit $\mathrm{UL}^{\alpha}_{\mathrm{WPERI}}$ for the WPERI can be obtained from Eq. (19). For every damaged beam, the histogram can be drawn when the $\mathrm{UL}^{\alpha}_{\mathrm{WPERI}}$ value is subtracted from the WPERI values. The damage location can be intuitively shown in histograms. Those histograms of four damaged beams are shown in Fig. 7. In Fig. 7(a), for instance, it can be seen that the wavelet packet energy rate indices appeared between nodes 14, 15 and 16, which

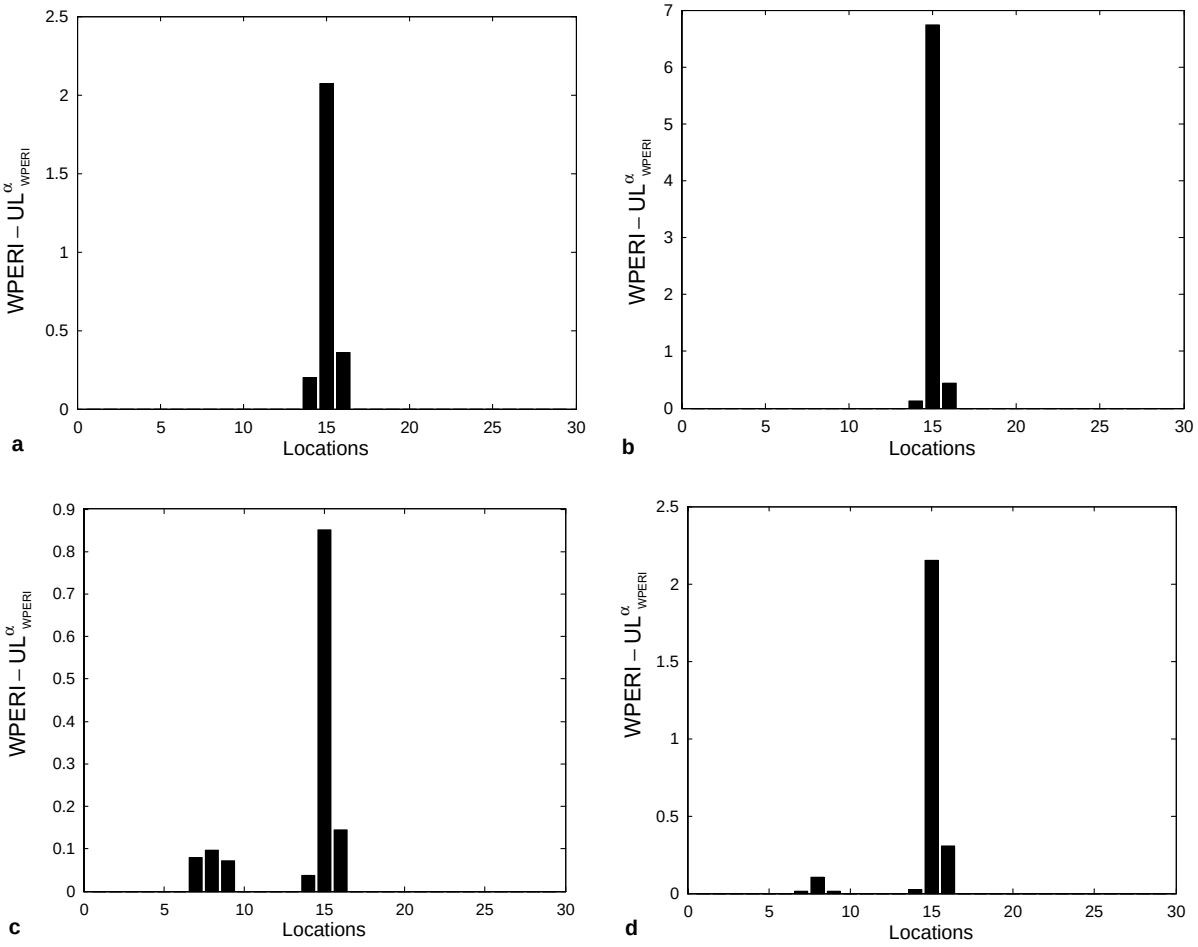

Fig. 7. Histograms of four damaged scenarios: (a) Beam-D1, (b) Beam-D2, (c) Beam-D3 and (d) Beam-D4.

are exactly the damage locations of bean D1. In Fig. 7(c), it can be observed that the wavelet packet energy rate indices appeared between nodes 7, 8, 9, 14, 15 and 16, which are identical to the damage location of beam D3. It is demonstrated that the locations of four damaged beams can be correctly identified.

Unfortunately, the damage severity cannot be identified quantificationally. However, for the same damage locations but different levels of damage compared with Fig. 7(a) and (b) or (c) and (d), the amplitude levels in the histograms are higher for the cases of more severe damage, which can represent the damage severity to some extent.

6. Tested beams in laboratory

To make the damage identification practical, the proposed damage identification procedure should be verified not only with the simulated data, but also with real measurement data from dynamic tests on the structures where the noise and measurement errors are present. The damage indices in most of

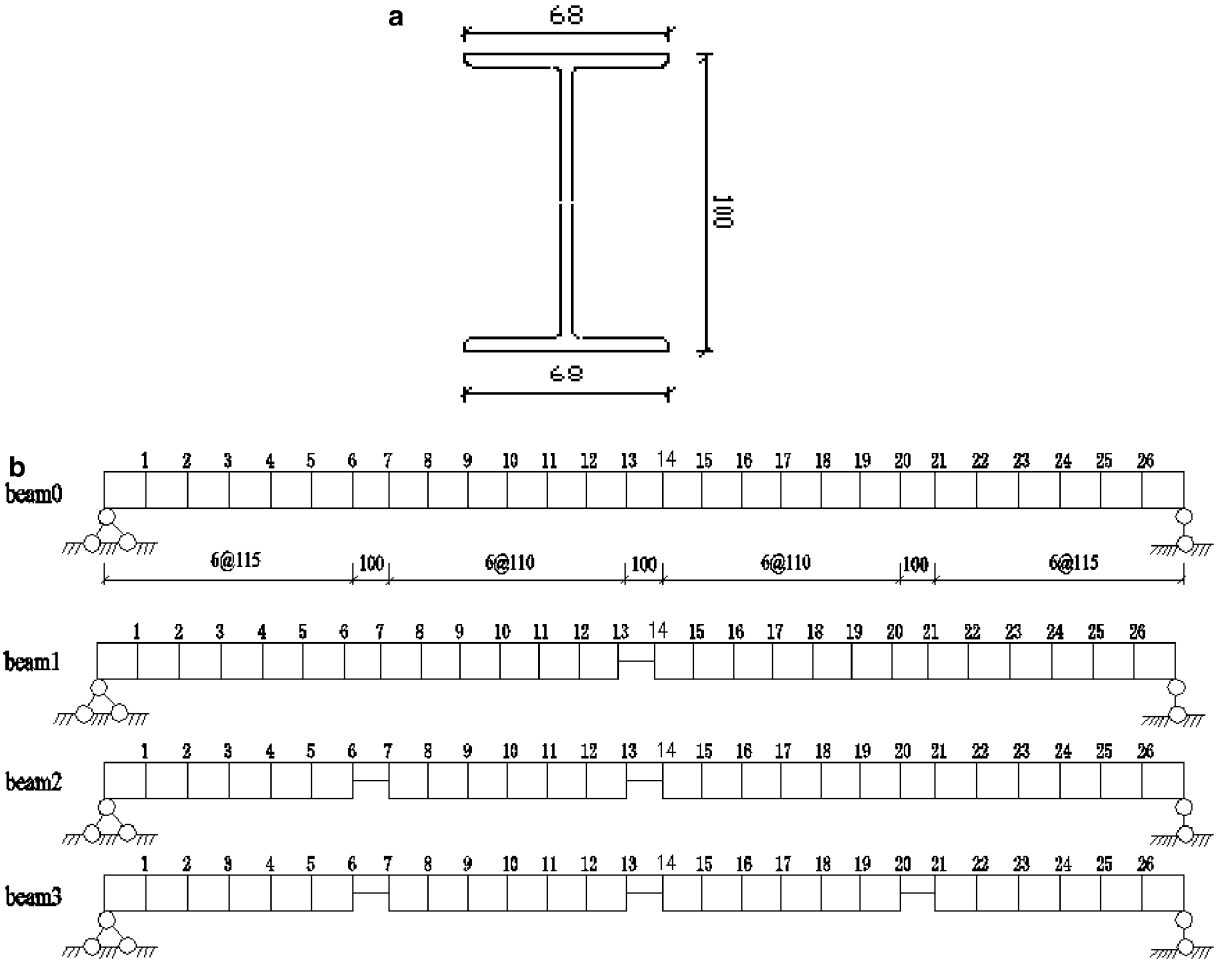

Fig. 8. Tested beams. (a) Cross section of tested beams. (b) Dimension and damage locations of tested beams.

modal-based dynamic identification techniques are sensitive to noise and measurement errors, which is the main difficulty for practical applications.

Four *I*-section steel beams with span length of 3 m, as shown in Fig. 8, are used to illustrate the proposed damage assessment index. Beam0 is an undamaged beam used as the reference. Beam1 is a one-damage scenario damaged at the middle of beam. Beam2 is a two-damage scenario where there are two damage locations. Beam3 is a three-damage scenario where there are three damage locations. All beams are dismembered 27 segments as shown in Fig. 8(b). The properties of the beams are as follows: mass density $\rho = 7117\ \mathrm{kg/m^3}$, elastic modulus $E = 210\ \mathrm{GN/m^2}$, cross section area $A = 14.33\ \mathrm{cm^2}$, and the inertia moment of cross section $I_x = 245\ \mathrm{cm^4}$, $I_y = 32.8\ \mathrm{cm^4}$.

Dynamic tests and measurements have been carried out on all the beams in the laboratory as shown in Fig. 9. The excitation is provided by an impact hammer applied at the center between 1 and 2 nodes. Twenty-six measurement locations as shown in Fig. 8(b) were measured by 3 setups. The force-balance accelerometers are used to measure the dynamic responses. The sampling frequency for all signals is 3000 Hz. The acceleration responses of all four beams at the same node (node 10) were shown in Fig. 10. It is observed that damage cannot been seen from the time history responses.

Fig. 9. Beam dynamic measurements in the laboratory.

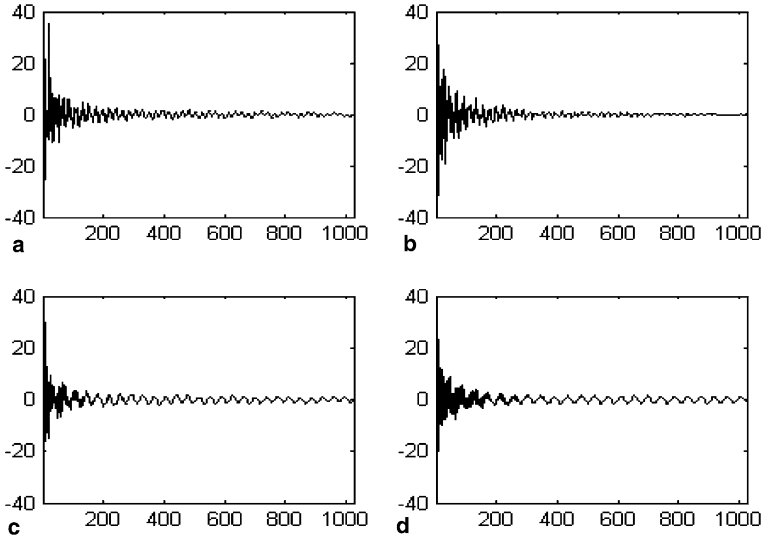

Fig. 10. Time-history signals recorded by the accelerometers.

As illustrated in simulated example, for the tested beams, the decomposition level is chosen to be 5 where a total of 32 component energies are generated. After decomposing the signals, the WPERIs $\Delta(E_{f_j})$ of every node are calculated using Eq. (18). These WPERIs $\Delta(E_{f_j})$ are shown in Fig. 11 for all damaged beams. Similarly, assuming $\alpha = 0.02$, the one sided 98% confidence upper limit $\mathrm{UL}^{\alpha}_{\mathrm{WPERI}}$ for the WPERIs can be calculated from Eq. (19). For every damaged beam, the histogram can be drawn when the $\mathrm{UL}^{\alpha}_{\mathrm{WPERI}}$ value is subtracted from the WPERI values. The histograms of three damaged beams are shown in Fig. 12. The damage location can be seen very clearly in these histograms. In the case of Beam1 in Fig. 12, for instance, it is clearly shown that (WPERI-$\mathrm{UL}^{\alpha}_{\mathrm{WPERI}}$) reaches the extreme in the location between nodes 13 and 14, which is exactly the damage location of Beam1. All results have demonstrated that the locations of three damaged beams can be identified from the real acceleration measurements.

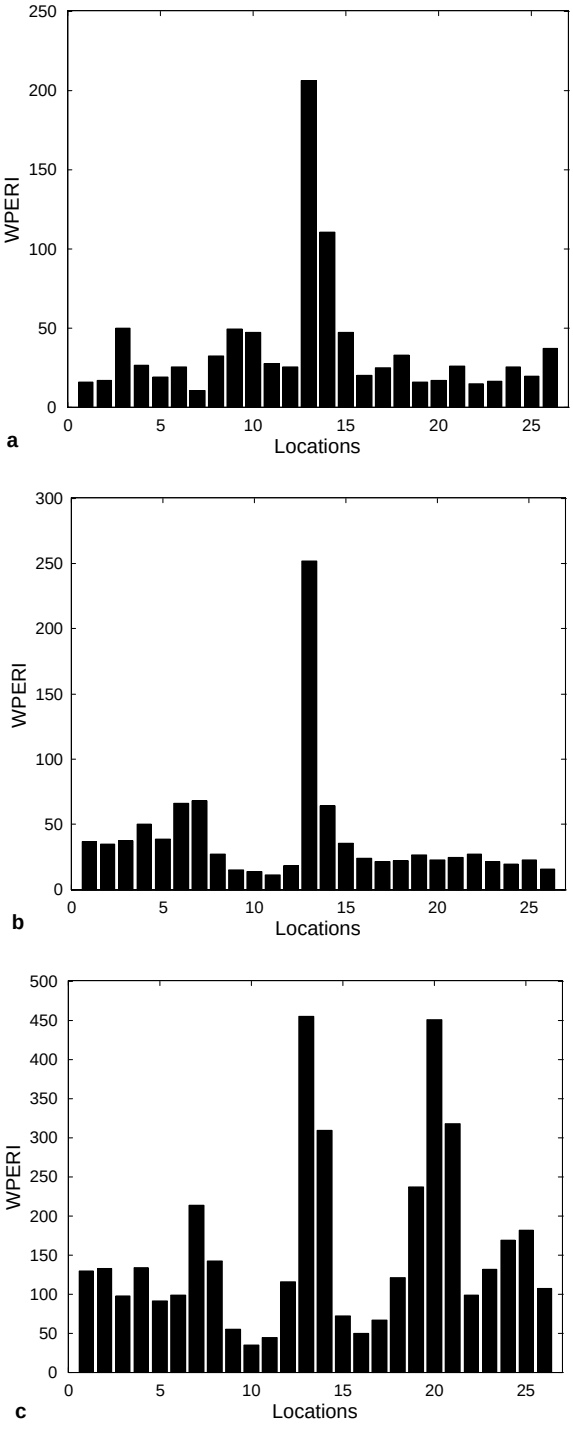

Fig. 11. Histograms of wavelet packet energy rate index: (a) Beam1, (b) Beam2 and (c) Beam3.

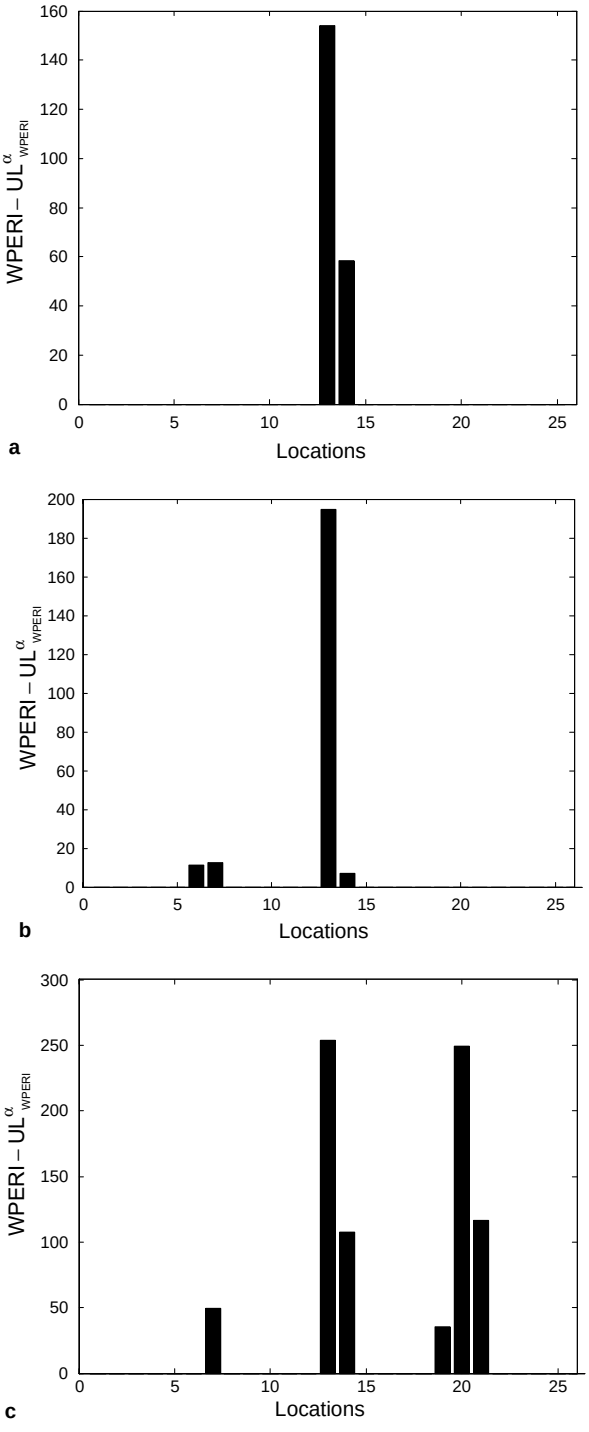

Fig. 12. Histograms after considering damage threshold: (a) Beam1, (b) Beam2 and (c) Beam3.

7. Concluding remarks

Wavelet transformation has emerged recently as a powerful mathematical tool for capturing change of structural characteristic induced by damage. Based on the analysis results of the simulated and tested beams, it is demonstrated that the proposed WPT-based energy rate index is a good candidate index that is sensitive to structural local damage. The tested beam verification through the real measurement data is of particular interest since noise or measurement errors are present in the signals and huge data are involved, which makes the proposed damage identification procedure practical. With regard to selecting the decomposition level, the lower decomposition level which can correctly identify the damage location is important since the lower decomposition level will reduce the computation efforts.

From the viewpoint of implementation, the proposed damage identification procedure requires three steps of computation: (1) wavelet packet decomposition; (2) wavelet packet energy rate calculation; and (3) damage location identification. These calculations are rather straightforward and not time-consuming, hence on-line implementation is possible if the reference information is available.

Although the proposed damage identification methodology has shown great potential in simulated and the laboratory tested beams, an important limitation of current method is that a reliable reference structural model for healthy (undamaged) conditions is required. As a signal based damage detection technique, the algorithm can detect damage when a sensor is placed at a damaged location. Further work is needed to make it applicable to large structural system where such circumstances are not possible. There are still some practical aspects that should be studied so that the wavelet packet based damage identification method can be applied to real structures.

Acknowledgement

The second author greatly acknowledges the financial fund supported by Program for New Century Excellent Talents (NCET) in University, Ministry of Education, People's Republic of China.

References

Ang, A.H.S., Tang, W.H., 1975. Probability Concepts in Engineering Planning and Design, vol. I. John Wiley & Sons, Inc., New York.

ANSYS®, 1999. User's manual, revision 5.6. Swanson Analysis System, USA.

Benffey, J.P., 1993. An Introduction to Reliability and Quality Engineering. Longman Scientific & Technical, Longman Group UK Limited, London.

Coifman, R.R., Wickerhauser, M.V., 1992. Entropy-based algorithms for best basis selection. IEEE Transactions of Information Theory 38, 713–718.

Daubechies, I., 1992. Ten Lectures on Wavelets. CBMS-NSF Regional Conference Series in Applied Mathematics. Dept. of Mathematics, Univ. of Lowell, MA, Society for Industrial and Applied Mathematics, Philadelphia.

Doebling, S.W., Farrar, C.R., Prime, M.B., 1998. A summary review of vibration-based damage identification methods. Shock and Vibration Digest 30 (2), 91–105.

Farrar, C.R., Doebling, S.W., Duffey, T.A., 1999. Vibration-based damage detection. In: SD2000, Struct. Dyn. Forum.

Gabor, D., 1946. Theory of communication. IEEE Journal 21, 149–157.

Gurley, K., Kareem, A., 1999. Application of wavelet transform in earthquake, wind and ocean engineering. Engineering Structures 21, 149–167.

Hou, Z., Noori, M., St. Amand, R., 2000. Wavelet-based approach for structural damage detection. Journal of Structural Engineering, ASCE 12 (7), 677–683.

Kitada, Y., 1998. Identification of nonlinear structural dynamic systems using wavelets. Journal of Engineering Mechanics, ASCE 124 (10), 1059–1066.

Mallat, S., 1989. A theory for multiresolution signal decomposition: The wavelet representation. IEEE Transactions on Pattern Analysis and Machine Intelligence 11, 674–693.

Montgomery, D.C., 1996. Introduction to Statistical Quality Control, third ed. Wiley, New York.
Ovanesova, A.V., Suarez, L.E., 2003. Application of wavelet transforms to damage detection in frame structures. Engineering Structures 26, 39–49.
Ren, W.X., De Roeck, G.., 2002a. Structural damage identification using modal data. I: Simulation verification. Journal of Structural Engineering, ASCE 128 (1), 87–95.
Ren, W.X., De Roeck, G.., 2002b. Structural damage identification using modal data. II: Test verification. Journal of Structural Engineering, ASCE 128 (1), 96–104.
Sohn, H., Czarnecki, J.A., Farrar, C.R., 2000. Structural health monitoring using statistical process control. Journal of Structural Engineering, ASCE 126 (11), 1356–1363.
Sun, Z., Chang, C.C., 2002. Structural damage assessment based on wavelet packet transform. Journal of Structural Engineering, ASCE 128 (10), 1354–1361.
Sun, Z., Chang, C.C., 2004. Statistical wavelet-based method for structural health monitoring. Journal of Structural Engineering, ASCE 130 (7), 1055–1062.
Wang, Q., Deng, X., 1999. Damage detection with spatial wavelets. International Journal of Solids and Structures 36 (23), 3443–3468.
Wang, W.J., McFadden, P.D., 1996. Application of wavelets to gearbox vibration signals for fault detection. Journal of Sound and Vibration 192 (5), 927–939.
Yen, G.G., Lin, K.C., 2000. Wavelet packet feature extraction for vibration monitoring. IEEE Transactions on Industrial Electronics 47 (3), 650–667.